Title
High-resolution visualization of mouse cardiac microvasculature using optical histology.

Journal
Biomedical Optics Express, 5(1)

ISSN
2156-7085

Authors
Moy, Austin J
Lo, Patrick C
Choi, Bernard

Publication Date
2014

DOI
10.1364/boe.5.000069

Peer reviewed

Biomedical Optics EXPRESS

High-resolution visualization of mouse cardiac microvasculature using optical histology

Austin J. Moy, Patrick C. Lo, and Bernard Choi*

Beckman Laser Institute, University of California, Irvine, 1002 Health Sciences Road East, Irvine, CA, USA
Department of Biomedical Engineering, University of California, Irvine, 3120 Natural Sciences II, Irvine, CA, USA
Edwards Lifesciences Center for Advanced Cardiovascular Technology, University of California, Irvine, CA, USA
*choib@uci.edu

Abstract: Cardiovascular disease typically is associated with dysfunction of the coronary vasculature and microvasculature. The study of cardiovascular disease typically involves imaging of the large coronary vessels and quantification of cardiac blood perfusion. These methods, however, are not well suited for imaging of the cardiac microvasculature. We used the optical histology method, which combines chemical optical clearing and optical imaging, to create high-resolution, wide-field maps of the cardiac microvasculature in ventral slices of mouse heart. We have demonstrated the ability of the optical histology method to enable wide-field visualization of the cardiac microvasculature in high-resolution and anticipate that optical histology may have significant impact in studying cardiovascular disease.

OCIS codes: (170.0170) Medical optics and biotechnology; (170.3880) Medical and biological imaging; (170.6930) Tissue; (170.1790) Confocal microscopy; (000.1430) Biology and medicine.

References and links

1. A. S. Go, D. Mozaffarian, V. L. Roger, E. J. Benjamin, J. D. Berry, W. B. Borden, D. M. Bravata, S. Dai, E. S. Ford, C. S. Fox, S. Franco, H. J. Fullerton, C. Gillespie, S. M. Hailpern, J. A. Heit, V. J. Howard, M. D. Huffman, B. M. Kissela, S. J. Kittner, D. T. Lackland, J. H. Lichtman, L. D. Lisabeth, D. Magid, G. M. Marcus, A. Marelli, D. B. Matchar, D. K. McGuire, E. R. Mohler, C. S. Moy, M. E. Mussolino, G. Nichol, N. P. Paynter, P. J. Schreiner, P. D. Sorlie, J. Stein, T. N. Turan, S. S. Virani, N. D. Wong, D. Woo, and M. B. Turner; American Heart Association Statistics Committee and Stroke Statistics Subcommittee, "Heart disease and stroke statistics--2013 update: a report from the American Heart Association," Circulation **127**(1), e6–e245 (2013).
2. A. C. Lardo, M. A. Cordeiro, C. Silva, L. C. Amado, R. T. George, A. P. Saliaris, K. H. Schuleri, V. R. Fernandes, M. Zviman, S. Nazarian, H. R. Halperin, K. C. Wu, J. M. Hare, and J. A. Lima, "Contrast-enhanced multidetector computed tomography viability imaging after myocardial infarction: characterization of myocyte death, microvascular obstruction, and chronic scar," Circulation **113**(3), 394–404 (2006).
3. T. H. Schindler, H. R. Schelbert, A. Quercioli, and V. Dilsizian, "Cardiac PET imaging for the detection and monitoring of coronary artery disease and microvascular health," JACC Cardiovasc. Imaging **3**(6), 623–640 (2010).
4. K. Wei, A. R. Jayaweera, S. Firoozan, A. Linka, D. M. Skyba, and S. Kaul, "Quantification of myocardial blood flow with ultrasound-induced destruction of microbubbles administered as a constant venous infusion," Circulation **97**(5), 473–483 (1998).
5. J. R. Panting, P. D. Gatehouse, G. Z. Yang, F. Grothues, D. N. Firmin, P. Collins, and D. J. Pennell, "Abnormal subendocardial perfusion in cardiac syndrome X detected by cardiovascular magnetic resonance imaging," N. Engl. J. Med. **346**(25), 1948–1953 (2002).
6. R. Nijveldt, M. B. Hofman, A. Hirsch, A. M. Beek, V. A. Umans, P. R. Algra, J. J. Piek, and A. C. van Rossum, "Assessment of microvascular obstruction and prediction of short-term remodeling after acute myocardial infarction: cardiac MR imaging study," Radiology **250**(2), 363–370 (2009).
7. W. L. Proudfit, E. K. Shirey, and F. M. Sones, Jr., "Selective cine coronary arteriography. Correlation with clinical findings in 1,000 patients," Circulation **33**(6), 901–910 (1966).
8. D. Eitzman, Z. al-Aouar, H. L. Kanter, J. vom Dahl, M. Kirsh, G. M. Deeb, and M. Schwaiger, "Clinical outcome of patients with advanced coronary artery disease after viability studies with positron emission tomography," J. Am. Coll. Cardiol. **20**(3), 559–565 (1992).
9. E. M. Geltman, D. Biello, M. J. Welch, M. M. Ter-Pogossian, R. Roberts, and B. E. Sobel, "Characterization of nontransmural myocardial infarction by positron-emission tomography," Circulation **65**(4), 747–755 (1982).

#195013 - $15.00 USD Received 2 Aug 2013; revised 4 Oct 2013; accepted 15 Nov 2013; published 4 Dec 2013

10. K. L. Gould, R. A. Goldstein, N. A. Mullani, R. L. Kirkeeide, W. H. Wong, T. J. Tewson, M. S. Berridge, L. A. Bolomey, R. K. Hartz, R. W. Smalling, F. Fuentes, and A. Nishikawa, "Noninvasive assessment of coronary stenoses by myocardial perfusion imaging during pharmacologic coronary vasodilation. VIII. Clinical feasibility of positron cardiac imaging without a cyclotron using generator-produced rubidium-82," J. Am. Coll. Cardiol. **7**(4), 775–789 (1986).
11. S. E. Nissen, J. C. Gurley, C. L. Grines, D. C. Booth, R. McClure, M. Berk, C. Fischer, and A. N. DeMaria, "Intravascular ultrasound assessment of lumen size and wall morphology in normal subjects and patients with coronary artery disease," Circulation **84**(3), 1087–1099 (1991).
12. B. N. Potkin, A. L. Bartorelli, J. M. Gessert, R. F. Neville, Y. Almagor, W. C. Roberts, and M. B. Leon, "Coronary artery imaging with intravascular high-frequency ultrasound," Circulation **81**(5), 1575–1585 (1990).
13. J. M. Tobis, J. Mallery, D. Mahon, K. Lehmann, P. Zalesky, J. Griffith, J. Gessert, M. Moriuchi, M. McRae, and M. L. Dwyer, "Intravascular ultrasound imaging of human coronary arteries in vivo. Analysis of tissue characterizations with comparison to in vitro histological specimens," Circulation **83**(3), 913–926 (1991).
14. E. A. Zerhouni, D. M. Parish, W. J. Rogers, A. Yang, and E. P. Shapiro, "Human heart: tagging with MR imaging--a method for noninvasive assessment of myocardial motion," Radiology **169**(1), 59–63 (1988).
15. P. G. Camici and F. Crea, "Coronary microvascular dysfunction," N. Engl. J. Med. **356**(8), 830–840 (2007).
16. C. A. Molyneux, M. C. Glyn, and B. J. Ward, "Oxidative stress and cardiac microvascular structure in ischemia and reperfusion: the protective effect of antioxidant vitamins," Microvasc. Res. **64**(2), 265–277 (2002).
17. G. M. Kazanskaia, A. M. Volkov, T. M. D'iakonitsa, and A. M. Karas'kova, "Ultrastructure of coronary microvessels in conditions of heart reperfusion following prolonged ischemia while applying various methods of artificial hypothermia," Tsitologiia **53**(12), 968–977 (2011).
18. K. Rakusan, N. Cicutti, and F. Kolar, "Cardiac function, microvascular structure, and capillary hematocrit in hearts of polycythemic rats," Am. J. Physiol. Heart Circ. Physiol. **281**(6), H2425–H2431 (2001).
19. J. C. Russell and S. D. Proctor, "Small animal models of cardiovascular disease: tools for the study of the roles of metabolic syndrome, dyslipidemia, and atherosclerosis," Cardiovasc. Pathol. **15**(6), 318–330 (2006).
20. A. R. Pries, H. Habazettl, G. Ambrosio, P. R. Hansen, J. C. Kaski, V. Schächinger, H. Tillmanns, G. Vassalli, I. Tritto, M. Weis, C. de Wit, and R. Bugiardini, "A review of methods for assessment of coronary microvascular disease in both clinical and experimental settings," Cardiovasc. Res. **80**(2), 165–174 (2008).
21. S. Lee, C. Vinegoni, P. F. Feruglio, L. Fexon, R. Gorbatov, M. Pivoravov, A. Sbarbati, M. Nahrendorf, and R. Weissleder, "Real-time in vivo imaging of the beating mouse heart at microscopic resolution," Nat Commun **3**, 1054 (2012).
22. J. Jones, R. Chowdhury, D. Jalloh, B. K. Seo, J. K. Pandya, C. B. Schaffer, and N. Nishimura, "In-Vivo Imaging of Beating Mouse Heart with Multiphoton Microscopy " in *Frontiers in Optics*(OSA, Rochester, NY, 2012), p. FM4D.6.
23. Y. S. Mukouyama, J. James, J. Nam, and Y. Uchida, "Whole-mount confocal microscopy for vascular branching morphogenesis," Methods Mol. Biol. **843**, 69–78 (2012).
24. J. Nam, I. Onitsuka, J. Hatch, Y. Uchida, S. Ray, S. Huang, W. Li, H. Zang, P. Ruiz-Lozano, and Y. S. Mukouyama, "Coronary veins determine the pattern of sympathetic innervation in the developing heart," Development **140**(7), 1475–1485 (2013).
25. J. A. Scherschel and M. Rubart, "Cardiovascular imaging using two-photon microscopy," Microsc. Microanal. **14**(6), 492–506 (2008).
26. V. Caorsi, C. Toepfer, M. B. Sikkel, A. R. Lyon, K. MacLeod, and M. A. Ferenczi, "Non-linear optical microscopy sheds light on cardiovascular disease," PLoS ONE **8**(2), e56136 (2013).
27. J. W. Verjans, D. Lovhaug, N. Narula, A. D. Petrov, B. Indrevoll, E. Bjurgert, T. B. Krasieva, L. B. Petersen, G. M. Kindberg, M. Solbakken, A. Cuthbertson, M. A. Vannan, C. P. Reutelingsperger, B. J. Tromberg, L. Hofstra, and J. Narula, "Noninvasive imaging of angiotensin receptors after myocardial infarction," JACC Cardiovasc. Imaging **1**(3), 354–362 (2008).
28. A. J. Moy, M. P. Wiersma, and B. Choi, "Optical histology: a method to visualize microvasculature in thick tissue sections of mouse brain," PLoS ONE **8**(1), e53753 (2013).
29. Y. Li, Y. Song, L. Zhao, G. Gaidosh, A. M. Laties, and R. Wen, "Direct labeling and visualization of blood vessels with lipophilic carbocyanine dye DiI," Nat. Protoc. **3**(11), 1703–1708 (2008).
30. D. J. Ravnic, X. Jiang, T. Wolloscheck, J. P. Pratt, H. Huss, S. J. Mentzer, and M. A. Konerding, "Vessel painting of the microcirculation using fluorescent lipophilic tracers," Microvasc. Res. **70**(1-2), 90–96 (2005).
31. S. M. White, S. C. George, and B. Choi, "Automated computation of functional vascular density using laser speckle imaging in a rodent window chamber model," Microvasc. Res. **82**(1), 92–95 (2011).
32. R. K. Jain, L. L. Munn, and D. Fukumura, "Measuring angiogenesis and hemodynamics in mice," Cold Spring Harb Protoc **2013**(4), 354–358 (2013).
33. J. E. Brush, Jr., R. O. Cannon 3rd, W. H. Schenke, R. O. Bonow, M. B. Leon, B. J. Maron, and S. E. Epstein, "Angina due to coronary microvascular disease in hypertensive patients without left ventricular hypertrophy," N. Engl. J. Med. **319**(20), 1302–1307 (1988).
34. G. A. Lanza and F. Crea, "Primary coronary microvascular dysfunction: clinical presentation, pathophysiology, and management," Circulation **121**(21), 2317–2325 (2010).
35. J. Herrmann, J. C. Kaski, and A. Lerman, "Coronary microvascular dysfunction in the clinical setting: from mystery to reality," Eur. Heart J. **33**(22), 2771–2782 (2012).

#195013 - $15.00 USD Received 2 Aug 2013; revised 4 Oct 2013; accepted 15 Nov 2013; published 4 Dec 2013

36. H. M. Arthur, P. Campbell, P. J. Harvey, M. McGillion, P. Oh, E. Woodburn, and C. Hodgson, "Women, cardiac syndrome X, and microvascular heart disease," Can. J. Cardiol. **28**(2 Suppl), S42–S49 (2012).
37. J. C. Kaski, "Overview of gender aspects of cardiac syndrome X," Cardiovasc. Res. **53**(3), 620–626 (2002).
38. S. E. Reis, R. Holubkov, A. J. Conrad Smith, S. F. Kelsey, B. L. Sharaf, N. Reichek, W. J. Rogers, C. N. Merz, G. Sopko, and C. J. Pepine, WISE Investigators, "Coronary microvascular dysfunction is highly prevalent in women with chest pain in the absence of coronary artery disease: results from the NHLBI WISE study," Am. Heart J. **141**(5), 735–741 (2001).
39. F. Leuschner and M. Nahrendorf, "Molecular imaging of coronary atherosclerosis and myocardial infarction: considerations for the bench and perspectives for the clinic," Circ. Res. **108**(5), 593–606 (2011).
40. I. Y. Chen and J. C. Wu, "Cardiovascular molecular imaging: focus on clinical translation," Circulation **123**(4), 425–443 (2011).

1. Introduction

The coronary vasculature is the network of cardiac blood vessels that delivers blood and other nutrients to the heart to maintain its normal function. A loss of blood flow to the heart due to dysfunction of the coronary vasculature leads to damage and death of the cardiac muscle cells, resulting in angina and ultimately myocardial infarction. Two closely related diseases cause dysfunction of the coronary vasculature: coronary artery disease (CAD) and coronary microvascular disease (CMVD). In 2010, this class of cardiovascular disease affected 15 million people in the United States alone [1]. Hence, considerable attention has been placed into understanding the pathology of cardiovascular disease that ultimately may enable prevention, diagnosis, and treatment.

Information about the cardiac vasculature can be either functional or structural. Functional information typically describes the blood perfusion in the heart, while structural information describes physiological changes in the vessel structure and organization. Methods to quantify blood perfusion in the heart include computed tomography [2], position emission tomography (PET) [3], ultrasound [4], and magnetic resonance imaging (MRI) [5,6]. Methods to visualize the cardiac vasculature include coronary angiography [7], PET [8–10], intravascular ultrasound [11–13], and MRI [14].

While these methods are suitable for imaging large coronary vessels and for quantifying cardiac blood perfusion, they are not well suited for imaging of the cardiac microvasculature. Visualization of the cardiac microvasculature is expected to enable understanding of changes that occur during development of cardiovascular disease. A standard method to directly visualize the cardiac microvasculature, either *in vivo* [15] or *ex vivo*, currently does not exist. To date, methods of visualizing the cardiac microvasculature primarily used electron microscopy [16,17] and histology [18], both of which enable visualization of the fine ultrastructure of *ex vivo* microvessels, but do not enable a wide-field view of the cardiac microvasculature.

Since cardiac imaging is primarily meant for clinical diagnosis, study of the cardiac microvasculature in humans is not practical. An alternative approach to visualization of the cardiac microvasculature and understanding the physiological changes that occur during cardiovascular disease, is to use preclinical animal models of cardiovascular disease [19,20]. Such models enable use of optical imaging methods that allow for high-resolution images of both the cardiac vasculature and microvasculature.

Previous studies employed confocal fluorescence microscopy [21–24] and multiphoton microscopy [21,22,25,26] to acquire depth-sectioned images of the cardiac microvasculature in mice. In these studies, cardiac microvasculature has been imaged both *in vivo* and in *ex vivo* harvested cardiac tissue. These methods were used to study the microvasculature after reperfusion after cardiac ischemia [21], to study the development of cardiac nerves in conjunction with cardiac vasculature in embryonic heart [24], to assess the degree of fibrosis after myocardial infarction [26], and to assess remodeling of the mouse heart and cardiac microvasculature after myocardial infarction [27]. These examples demonstrate that there is considerable interest in using optical imaging to investigate the cardiac vasculature in preclinical models.

#195013 - $15.00 USD Received 2 Aug 2013; revised 4 Oct 2013; accepted 15 Nov 2013; published 4 Dec 2013

We have developed a technique called optical histology [28] that enables high-resolution, depth-resolved visualization of tissue microvasculature. Our technique combines optical imaging with chemically-mediated optical clearing of the tissue, which reduces the optical scattering in the tissue, allowing both deeper penetration of excitation light and enhanced visualization of the microvascular network in the tissue. We demonstrate the use of optical histology to image the cardiac microvasculature in *ex-vivo* preclinical models of the heart and discuss how our technique may be used to image specific molecular targets in the heart and ultimately be used to study various cardiovascular diseases.

2. Methods

2.1 Optical histology

We previously described the optical histology imaging technique [28]. Using cardiac perfusion [29,30], we first injected the fluorescent agent DiI into the circulation. DiI is a lipophilic dye that diffuses into and embeds itself into the cell membrane of the endothelial cells lining the vascular wall.

We harvested the hearts from nine healthy male C3H mice and incubated them in 4% w/v paraformaldehyde, to fix the organs. We then sliced the hearts into thick tissue sections that are limited to the thickness of the heart wall (~400-500 μm). We immersed each section in FocusClear (CelExplorer Labs, Hsinchu, Taiwan), an optical clearing agent containing dimethyl sulfoxide, for three hours. In this report, we show representative data from three heart slices.

2.2 Tissue sample holder

After immersion in FocusClear, we placed the section into a purpose-built tissue holder, consisting of a 30-mm optic holder (CP08, Thor Labs, New Jersey, USA), two 25-mm circular cover glasses (Fisherbrand Cover Glass No.1, Fisher Scientific), and two 30-mm retaining rings (SM30RR, Thor Labs, New Jersey, USA) (Fig. 1). This holder fixed the sample position and ensured that the sample had a uniform thickness.

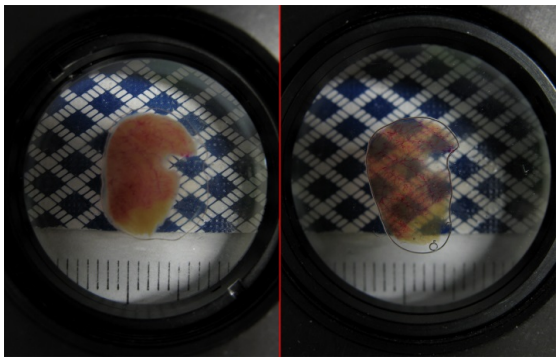

Fig. 1. Epi-illumination images of mouse heart sections (left) before and (right) after optical clearing with FocusClear. These images clearly depict the increased section transparency that results from optical clearing.

2.2 Confocal fluorescence microscopy

With a confocal fluorescence microscope (LSM Meta 510, Zeiss), we collected sequential z-stack images over the entire surface area of the tissue. We used a 10x microscope objective. Similar to the images in our previous study [28], we present the collected three-dimensional data set as depth-encoded, maximum intensity projection (MIP) images. In each image, each pixel is assigned a color corresponding to the depth in the z-stack at which the fluorescence emission signal is highest.

#195013 - $15.00 USD Received 2 Aug 2013; revised 4 Oct 2013; accepted 15 Nov 2013; published 4 Dec 2013

2.3 Nonlinear optical microscopy

We used the Zeiss Meta 510 microscope to image DAPI-stained nuclei in ventral slices of heart and intrinsic second harmonic signals from the tissue. We used 800-nm light and the principles of two-photon excited fluorescence, to excite DAPI. We used either a 20x objective or a 40x water immersion objective, and collected fluorescence emission with a 390-465 nm bandpass filter.

2.4 Image analysis

Using an algorithm described by White et al. [31], we calculated functional vascular density (FVD) in select regions of interest. FVD is commonly used in studies of angiogenesis [32], to quantify vessel density, and is the total length of vessels in the imaged region of interest, divided by the area of the region. Briefly, our FVD algorithm thresholds the image by criteria related to pixel intensity and vessel size, and then skeletonizes the image. Based on the skeletonized data in the region of interest, the algorithm calculates the FVD of the region.

3. Results

Figure 1 shows a ventral slice of mouse heart both (a) before and (b) after 3 hours of optical clearing that has been mounted in the tissue sample holder. The tissue slice appears noticeably more transparent after optical clearing, and the larger DiI-labeled cardiac vessels are visible to the naked eye after optical clearing.

Figure 2 shows a MIP image of a DiI-labeled heart slice (a) before and (b) after optical clearing. While the imaging depth is the same (460 μm), the increased section transparency that results from optical clearing enhances the vascular density that can be visualized by a factor of 1.5-2.0.

Figure 3 shows the region of microvasculature in Fig. 2(B) enclosed by the green line. A large coronary vessel is visible in this image, running diagonally across from the lower left to upper right, along with a dense network of microvessels surrounding the coronary vessel. Such images demonstrate the detailed maps of the cardiac microvasculature that the optical histology method can provide.

Figure 4 shows representative DiI-labeled dorsal and ventral heart slices. These slices were imaged after optical clearing and demonstrate the repeatability of the optical histology technique. The slice in (a) was imaged to a depth of 560 μm while the slice in (b) was imaged to a depth of 540 μm. The imaging depth is similar to that of the slice in Fig. 2.

Figure 5 shows the DiI-labeled mouse cardiac microvasculature in a ventral heart slice after optical clearing. For this slice, the nuclei also were counter-stained with DAPI. This image shows the ability of optical histology to image multiple tissue markers simultaneously and demonstrates the potential of optical histology to be used with molecular markers for structures of interest other than the microvasculature.

Table 1 is a summary of the FVD calculated in 1) nine different regions of interest (ROIs) in both the native (Fig. 2(A)) and optically-cleared (Fig. 2(B)) heart slices seen, as well as the heart slices shown in Fig. 4. The FVD of the bottom left and bottom center regions of the heart slice in Fig. 2, corresponding to ischemic regions of the heart, is substantially less than the other perfused regions of the heart which is consistent with a qualitative assessment of the region in Fig. 2.

#195013 - $15.00 USD Received 2 Aug 2013; revised 4 Oct 2013; accepted 15 Nov 2013; published 4 Dec 2013

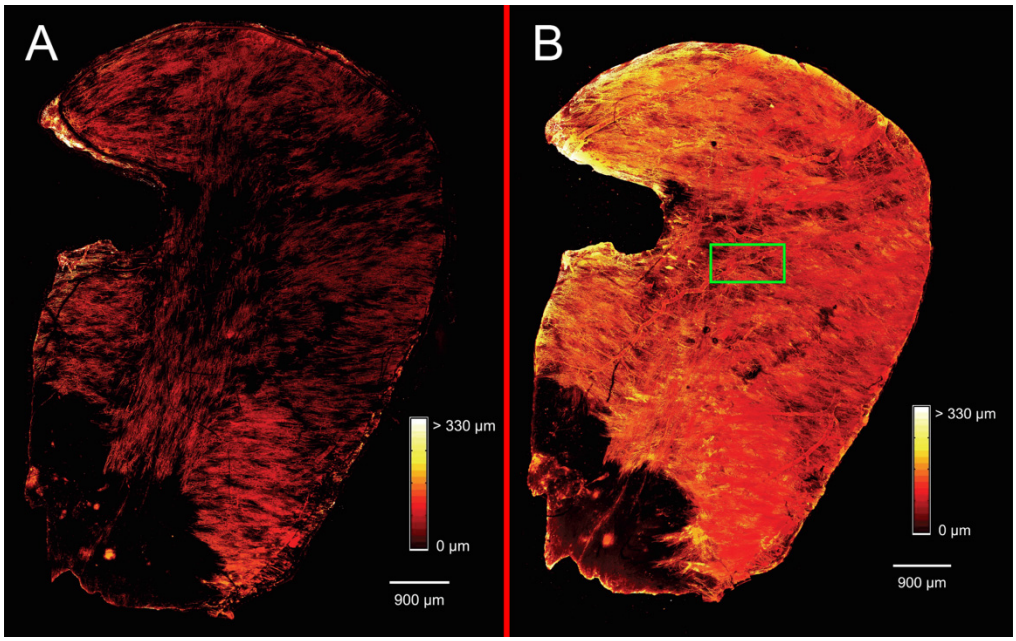

Fig. 2. MIP map of the cardiac microvasculature in a (a) native and (b) optically-cleared ventral heart slice. The colormap corresponds to the depth of maximum signal at each pixel, and is the same for both images. The imaging depth does not increase substantially due to the relative thinness of the tissue, however, the vascular density is much more pronounced. Region outlined in green is shown in Fig. 3.

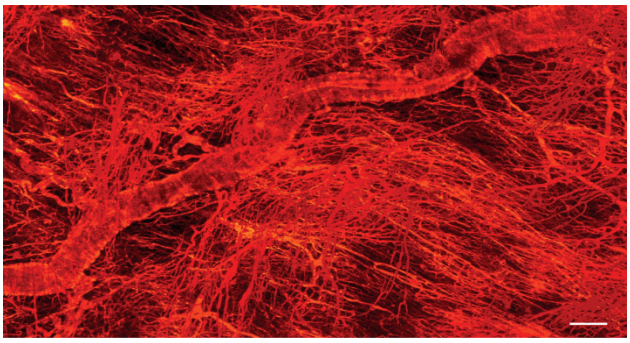

Fig. 3. Region outlined in green in Fig. 2(B) showing zoomed in view of coronary vessel and microvasculature acquired at 10x magnification. Scale bar is 100 µm.

#195013 - $15.00 USD Received 2 Aug 2013; revised 4 Oct 2013; accepted 15 Nov 2013; published 4 Dec 2013

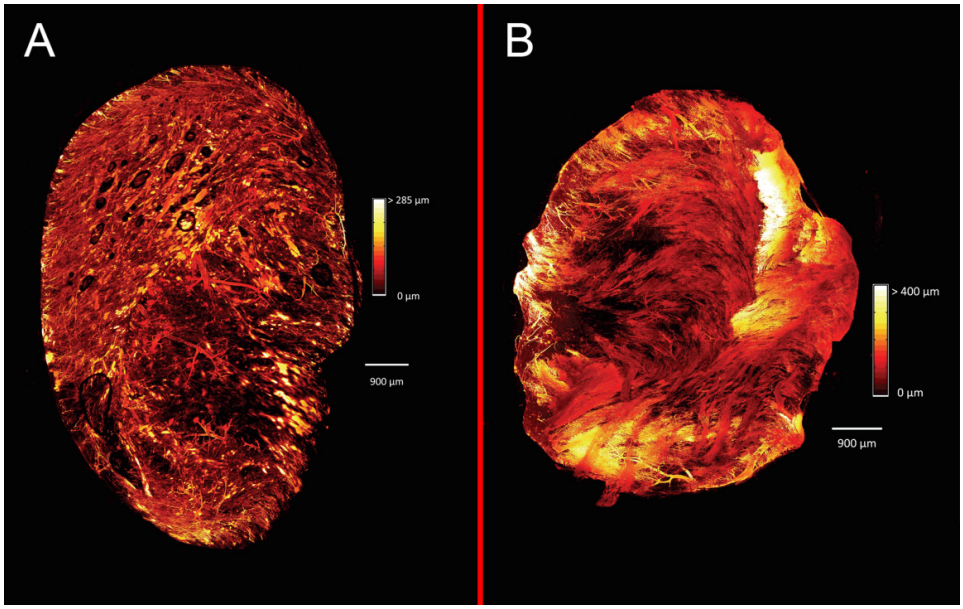

Fig. 4. MIP map of representative ventral slices of mouse heart after optical clearing.

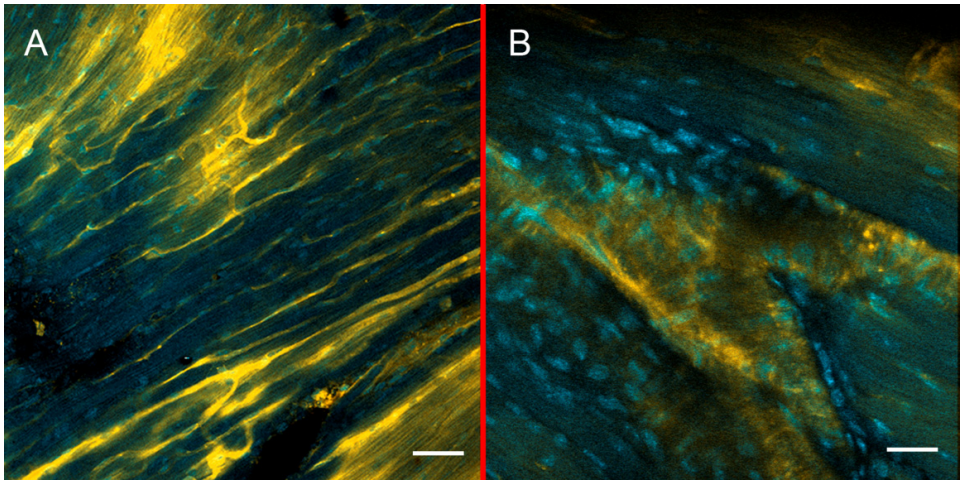

Fig. 5. Optical histology enables imaging of multiple markers of interest. Images were acquired at (a) 20x and (b) 40x magnification of mouse cardiac microvasculature labeled with DiI and nuclei counter stained with DAPI. Scale bar for (a) is 50 µm and (b) 25 µm.

Table 1. FVD calculations of select regions of interest of the heart slices in Fig. 2 and Fig. 4

Heart Slice ROI	Figure 2(A) FVD, cm^{-1}	Figure 2(B) FVD, cm^{-1}	Figure 4(A) FVD, cm^{-1}	Figure 4(B) FVD, cm^{-1}
Top left	521	857	443	671
Top center	588	907	404	645
Top right	401	855	374	704
Middle left	415	764	423	365
Middle center	449	837	374	780
Middle right	396	774	238	622
Bottom left	26	76	248	803
Bottom center	75	57	385	669
Bottom right	565	713	222	708

#195013 - $15.00 USD Received 2 Aug 2013; revised 4 Oct 2013; accepted 15 Nov 2013; published 4 Dec 2013

4. Discussion

The results demonstrate our ability to visualize the cardiac microvasculature with encoded depth information. Using our combined optical clearing and optical imaging techniques, we generated a detailed map of the microvasculature in ventral and dorsal slices of mouse heart (Fig. 2 and Fig. 4). We resolved 5-μm diameter capillaries in the tissue (Fig. 3), even at a relatively low 10x magnification. The use of optical clearing allowed us to substantially increase the density of visible cardiac microvasculature (Fig. 2, Table 1). We also demonstrated the applicability of our technique to quantify FVD in other heart slices from the ventral portion of the heart (Fig. 4). The FVD data (Table 1) of the three heart slices suggest the spatial heterogeneity in microvascular density in the cardiac tissue.

Of particular interest is the extremely high density of microvessels in the heart that we could visualize after optical clearing (Fig. 3). After optical clearing, the FVD of the slice in Fig. 2 increased approximately 1.5-2.0x as compared to the FVD visualized in uncleared tissue (Fig. 2(A)). In addition, the bottom left and bottom center regions of the section, which we believe were not perfused, had FVD values considerably lower than the other perfused regions of the heart. These data suggest the ability of optical histology to study heart ischemia and cardiac remodeling, and response of cardiac tissue to subsequent injury and therapy. The increase in FVD after optical clearing is further confirmed by the FVD calculations performed on the heart slice in Fig. 4(B), which has values that are similar to those from the heart slice in Fig. 2.

We further show that optical histology enables imaging of multiple tissue structures simultaneously. Figure 5 is a set of images acquired at 20x and 40x magnification with the microvasculature labeled with DiI (color coded yellow in the figure) with heart muscle cell nuclei counter-stained with DAPI (color coded blue in the figure). We accomplished this with combination of infusion of DiI into the microcirculation and DAPI staining of nuclei, prior to optical clearing of the heart slice. Excitation of DAPI fluorescence also enabled visualization of the DAPI-stained nuclei, as well as intrinsic second harmonic signals from the tissue. We believe that the latter, which was also collected in the same channel as the DAPI emission and is visible in the high magnification images, corresponds to the muscle fibers of the heart and originates from the myosin in the muscle fibers.

We believe that the ability of our optical histology technique to enable visualization of the highly dense network of cardiac microvasculature, may have a significant impact in studying cardiovascular disease, including CAD and especially CMVD [15, 33–35]. While CAD, which is the most prevalent form of cardiovascular disease and the leading cause of death in the United States [1], has received considerable attention, CMVD is a relatively underexplored area of research.

CMVD is a diagnosis in patients that present with angina but, after undergoing diagnostic tests for CAD, are shown to have clear coronary arteries that suggest a lack of CAD. CMVD, which is also called cardiac syndrome “X” [36,37], is characterized by dysfunction of the cardiac microvasculature and differs from CAD in that there is no plaque buildup in the microvasculature [34]. CMVD is estimated to affect three-million American women and is thought to be the primary cause of heart disease in women. Current knowledge about CMVD and how to treat it is limited; most of the knowledge about CMVD has been gained from a large clinical study initiated in the early 2000s [38].

Using our optical histology method, both CAD and CMVD could be further investigated in animal models of these diseases to study the changes in cardiac microvasculature that occur during disease progression and how they could best be treated. Another potential application of our optical histology technique is to investigate the effects of myocardial infarction on the cardiac microvasculature and may be especially useful in learning about the revascularization process that occurs during recovery from myocardial infarction. For example, in the bottom left corner of both the native and post-clearing MIP images in Fig. 2; the DiI fluorescent label

#195013 - $15.00 USD Received 2 Aug 2013; revised 4 Oct 2013; accepted 15 Nov 2013; published 4 Dec 2013

is largely absent from this region. Based on visual inspection of the heart prior to sectioning, we speculate that this region of the heart was ischemic. This speculation is supported by the lack of DiI fluorescent label in the region, which is an expected outcome associated with compromised blood flow to the region. Future studies are warranted to explore further the potential of ischemic region monitoring using controlled procedures (e.g., coronary artery ligation).

In addition, molecular targeting has received significant attention in cardiovascular research [39,40] and the images of cardiomyocyte nuclei in Fig. 5 show the potential of our method to image other specific molecular targets in addition to the vasculature, which could be very significant in investigating cardiovascular disease.

We have presented here data which demonstrate the ability of optical histology to achieved detailed, high-resolution visualization of the cardiac microvasculature. Our technique, which combines chemical optical clearing and optical microscopy, produces wide-field maps of the microvasculature in both the ventral and dorsal surfaces of the mouse heart by creating a mosaic of adjacent image stacks that span the entire cardiac tissue surface. We present these maps of the cardiac microvasculature as depth-encoded MIP images that give three-dimensional information in a two-dimensional image. We believe our technique will have significant utility in cardiovascular research and could be applied to the study the effects of CAD, CMVD, and myocardial infarction on the cardiac microvasculature.

Acknowledgments

The authors would like to acknowledge CelExplorer Labs (Hsinchu, Taiwan) for generously donating FocusClear, Dr. Tatiana Krasieva (University of California, Irvine), and Dr. Sean White (University of California, Irvine) for their support. This work was supported in part by the Arnold and Mabel Beckman Foundation, the Summer Undergraduate Research Program sponsored in part by the UC Irvine Edwards Lifesciences Center for Advanced Cardiovascular Technology, and National Institutes of Health grant awards R01HD065536 and P41EB015890. The content is solely the responsibility of the authors and does not necessarily represent the official views of the National Institutes of Health.

#195013 - $15.00 USD Received 2 Aug 2013; revised 4 Oct 2013; accepted 15 Nov 2013; published 4 Dec 2013